AD-A085 673 IBM THOMAS J WATSON RESEARCH CENTER YORKTOWN HEIGHTS NY F/G 20/12
SPECTROSCOPIC STUDIES OF THE ELECTRONIC STRUCTURE OF METAL-SEMI--ETC(U)
MAR 80 D E EASTMAN F44620-76-C-0041

UNCLASSIFIED AFOSR-TR-80-0455 NL

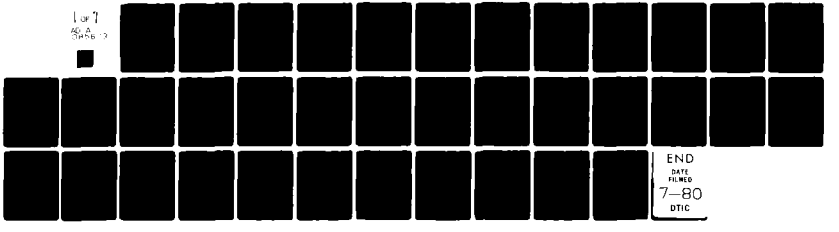

SPECTROSCOPIC STUDIES OF THE ELECTRONIC STRUCTURE OF METAL-SEMICONDUCTOR AND VACUUM-SEMICONDUCTOR INTERFACES

Dean E. Eastman

IBM Thomas J. Watson Research Center
P.O. Box 218
Yorktown Heights, New York 10598

March 24, 1980

Final Technical Report for the Period October 1, 1976 - October 31, 1979

Contract No. F44620-76-C-0041

Approved for public release, distribution unlimited.

Prepared for:

Air Force Office of Scientific Research(AFSC)
Bldg. 410, Bolling AFB, D.C. 20332

unclassified

SECURITY CLASSIFICATION OF THIS PAGE (When Data Entered)

REPORT DOCUMENTATION PAGE	READ INSTRUCTIONS BEFORE COMPLETING FORM
1. REPORT NUMBER: AFOSR-TR-80-0455	2. GOVT ACCESSION NO.: AD-A085 873	3. RECIPIENT'S CATALOG NUMBER
4. TITLE (and Subtitle): Spectroscopic Studies of the Electronic Structure of Metal-Semiconductor and Vacuum-Semiconductor Interfaces.	5. TYPE OF REPORT & PERIOD COVERED: Final 10/1/76 - 10/31/79
	6. PERFORMING ORG. REPORT NUMBER
7. AUTHOR(s): Dean E. Eastman	8. CONTRACT OR GRANT NUMBER(s): F44620-76-C-0041
9. PERFORMING ORGANIZATION NAME AND ADDRESS: IBM Thomas J. Watson Research Center, P. O. Box 218, Yorktown Heights, New York 10598	10. PROGRAM ELEMENT, PROJECT, TASK AREA & WORK UNIT NUMBERS: 61102F 2306/B2
11. CONTROLLING OFFICE NAME AND ADDRESS: Air Force Office of Scientific Research/NE (AFSC); Bldg. 410; Bolling AFB, D.C. 20332	12. REPORT DATE: March 24, 1980
	13. NUMBER OF PAGES: 36
14. MONITORING AGENCY NAME & ADDRESS(if different from Controlling Office)	15. SECURITY CLASS. (of this report): Unclassified
	15a. DECLASSIFICATION/DOWNGRADING SCHEDULE

16. DISTRIBUTION STATEMENT (of this Report)

Approved for public release; distribution unlimited.

Final rept. 1 Oct 76 - 31 Oct 79

17. DISTRIBUTION STATEMENT (of the abstract entered in Block 20, if different from Report)

18. SUPPLEMENTARY NOTES

19. KEY WORDS (Continue on reverse side if necessary and identify by block number)

Semiconductor Surfaces; Electronic Structure; Surface Physics; Experimental Energy Band Dispersions

20. ABSTRACT (Continue on reverse side if necessary and identify by block number)

The electronic structure and properties of semiconductor interfaces including both vacuum-semiconductor and metal-semiconductor interfaces as well as relevant metal and semiconductor materials have been investigated under this contract. The emphasis is on elucidating the electronic properties of these materials and their interfaces, e.g., metal-

DD FORM 1473

349250 unclassified

semiconductor Schottky barriers, which are of far reaching importance in such semiconductor devices as MOSFETS, CCD devices, photovoltaic devices, etc. ~~We have performed~~ extensive studies of the electronic structure of semiconductor surfaces and interfaces and related metal surfaces as a function of surface preparation, doping, thickness of adsorbed overlayer, etc. HAS BEEN PERFORMED. The probes we have used include photoelectron spectroscopy (XPS and UPS - with an emphasis on angle-resolved studies using synchrotron radiation) and yield spectroscopy, electron energy loss spectroscopy, low energy electron diffraction and theoretical band structure methods. Our research has included studies of well characterized surfaces of silicon and gallium arsenide, of silicides and Si-silicide interfaces, of bulk Ge, GaAs and GaSb, of Ni and Co surfaces, of bulk Ni, Cu, Fe, Co, ThH_2, Zn and LaB_6 materials. A major achievement of our research program has been the development for the first time of accurate experimental methods for determining the electron energy vs momentum band dispersions $E(\vec{k})$ of materials and their surfaces; such $E(\vec{k})$ dispersions are of central importance in solid state physics in understanding the electronic, physical and chemical properties of materials.

TABLE OF CONTENTS

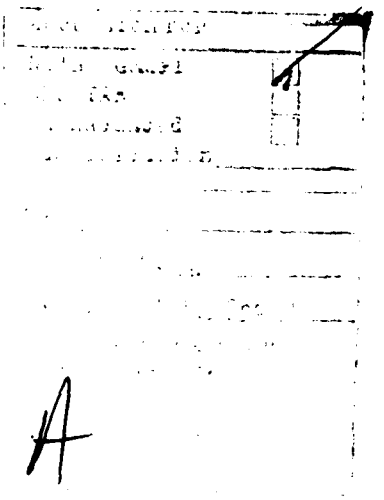

I. HIGHLIGHTS

Significant and extensive progress in understanding the electronic structure and properties of semiconductor surfaces and semiconductor interfaces as well as selected metallic and semiconductor materials has been accomplished under Air Force Office of Scientific Research Contract F44620-76-C-0041 [Oct.'75-Sept.'79]. Techniques which have been used include photoelectron spectroscopy (with an emphasis on angle-resolved photoemission using synchrotron radiation), low energy electron diffraction (LEED), electron energy loss spectroscopy and Auger spectroscopy, as well as realistic band structure calculations for surfaces and bulk materials. In summary, 34 research papers have been published under this contract (see Section III) on the electronic structure of (a) semiconductor surfaces and interfaces, (b) group IV and III-V semiconductors, (c) metal surfaces, (d) metals and metallic compounds, and (e) many-electron effects. As selected examples, three major highlights are described in this Section: (1) New instrumentation—a display analyzer system for photoemission, (2) band structure determination of semiconductor surfaces—Si(100)-(2×1) and (3) band structure determination of bulk semiconductors—GaAs. A major accomplishment of our research program has been the development for the first time of accurate experimental methods for determining the electron energy vs momentum $E(\vec{k})$ band dispersions of surfaces and bulk materials. Such one-electron band dispersions $E(\vec{k})$ are of central importance in solid state physics in understanding the physical, chemical and electronic properties of materials and their surfaces and interfaces.

Ellipsoidal Mirror Display Analyzer System for Electron Energy and Angular Measurements. A new type of electron energy analyzer[1] (Fig. 1) with full angular display (~ 2 steradians) has been conceived and constructed by D.E. Eastman at IBM which is successfully operating at the Synchrotron Radiation Center at the University of Wisconsin-Madison. This is the first display-type spectrometer and has, for many types of measurements, an unprecedented performance - better than 100 meV energy resolution and ~2° angular resolution with total data rates ~100 times greater than other spectrometers. The design and development were motivated by the objective of constructing a high-resolution analyzer system capable of the combined measurements of:

(1) angle-resolved XUV photoemission spectroscopy (ARPES) with a polarized synchrotron radiation source
(2) angle-integrated XUV photoemission spectroscopy
(3) efficient Auger electron spectroscopy (AES)
(4) low-energy electron diffraction (LEED).

The primary motivation was ARPES with synchrotron radiation, for which the differential photoemission cross section $N(E,h\nu,\mathbf{k},\hat{e}_p,\hat{n})$ involves the measurement/control of four continuous variables (electron energy E, photon energy $h\nu$, and two independent components of momentum $\vec{k}$, i.e., the angular direction) as well as the polarization $\hat{e}_p$ of the radiation and crystallographic direction $\hat{n}$ of the single crystal sample. This new display-type spectrometer system, which incorporates a separate UHV sample preparation chamber, has been combined with a novel TGM monochromator that covers the entire spectral range ($5 \lesssim h\nu \lesssim 150$ eV) of the 240 MeV storage ring radiation source at the University of Wisconsin-Madison. It has been used for several types of angle-resolved and angle-integrated electron spectroscopies — photoemission, Auger, energy loss as well as elastic and inelastic low energy electron diffraction (LEED and ILEED) for about two years with great success. This system has been of central importance in attaining a major achievement: the development of techniques for accurately determining one-electron band dispersions $E(\vec{k})$ for solids and surfaces. These results are summarized in Section III.

A description of the principles of operation and features of the electron imaging two-dimensional display spectrometer system, schematically shown in Fig. 1, is as follows. A top view is depicted in Fig. 1, with $h\nu$ denoting the radiation (horizontally polarized monochromatic synchrotron radiation) which enters through a hole in the ellipsoidal mirror at 34° below the horizontal plane, e-AES denotes an electron source (~ 1-2 keV) for Auger spectroscopy, and e-LEED denotes an electron source (0-400 eV) for LEED studies. Combined energy and angular analyses are achieved by using two retarding fields: an ellipsoidal mirror (V_r) used in a reflection mode as a low-pass energy filter, and a spherical 4-grid stage (retard grid shown, V_t) used in a transmission mode as a high-pass filter. With an energy overlap of the two filters for electrons emitted in any direction within the acceptance angle of the analyzer (3 directions shown), the analyzer transmits electrons only in a narrow energy range ΔE about the pass energy $E_p \simeq eV_t$. By suitably adjusting V_r and V_t, an energy resolution $\Delta E = 0.1$ eV or larger can be selected (~1mm diameter source size, E_p~10eV) while accepting the full solid angle. A two-dimensional position-sensitive detector stage follows the high pass filter. This consists of two continuous electron multiplier arrays (CEMA) with a gain of $\sim 10^7$ followed by a phosphor screen. The electron pulses (~2ns) leaving the CEMA are accelerated and converted to light pulses ($\sim 10^8$ photons/pulse) at the phosphor screen, which are viewed and recorded through a viewport. Electrons reaching the detector stage have a one-to-one relationship between their angular direction and detected position.

Two angle-resolved detectors for ARPES are used. Namely, the image on the screen is viewed through a viewport with a beam-splitting mirror while a second mirror and lens form an image of the screen (Fig. 1). There is a single-channel angle-resolved detector (acceptance $\delta\theta = 2°$-$35°$ full angle) which has an adjustable optical iris in this image plane (x and y coordinates and size are electronically-controlled) followed by a photomultiplier counting system. This detector views a selected direction and digitally counts all electron events within an acceptance angle $\delta\theta$. Counting rates are typically 10^4-10^5 c/s for $\delta\theta \simeq 4°$-$10°$, $\Delta E \simeq 0.1$-0.3 eV, and $h\nu$~8-50 eV.

The second angle-resolved detector is a two-dimensional digital data acquisition system which utilizes the full capability of the analyzer. As schematically shown in Fig. 1, this consists of a silicon-intensified-target (S.I.T.) video camera which records all electron events and reads them (video rates of ~3.5 megaband pixel rate) into a two-dimensional multichannel analyzer (2-D MCA) which is controlled by an IBM Series/1 computer system that collects, processes, and transfers data pictures to a Tektronix 4015 graphics terminal and to the IBM 370/168 computer system at IBM Research, Yorktown Heights, New York, over a 9600 baud line. The MCA (Quantex Model DS12) has $256 \times 256 = 65{,}536$ channels or pixels, each with a 12-bit word. Each channel, which corresponds to an angle of $\sim 1/3° \times 1/3°$, can be operated in a counting mode or a signal-averaging (ratemeter) mode. Energy distribution "pictures" (EDP's) can thus be taken and stored. Subsequently, angle-resolved energy distributions (AREDC's) for arbitrary directions can be selected from these "EDP's" and viewed. Angle-integrated spectra are simply obtained by summing all pixels of each full picture and plotting each picture sum versus electron energy.

Electronic Structure of Surfaces— $E(\vec{k})$ Band Dispersions for Si(100)-(2×1) Surface. The Si(100) surface is the standard substrate used for MOSFETS and has been studied extensively. When prepared with a clean surface, Si(100) reconstructs with a (2×1) surface unit mesh, as seen by low energy electron diffraction (LEED). The reconstructed Si(100)-(2×1) surface has been the subject of many theoretical studies and experimental studies, including photoemission,[2] LEED,[3] and electron energy loss spectroscopy. Various structural models have been proposed and studied for this reconstructed surface, including a number of different pairing models[3,5-8,11,12] and vacancy models.[5,6,8,10,12] Several different conclusions have been reached concerning the structure of the Si(100)(2×1) surface via calculations of LEED[3,12] and photoemission spectra[6,7] and comparison with experimental data. A "zig-zag"

chain model has been proposed which is based on a LEED intensity analysis;[3] a self-consistent surface calculation for this model yields metallic surface state bands.[7] Self-consistent surface calculations have also been performed for a vacancy model and a dimer-like pairing model,[6,8] as well as for the ideal unrelaxed and unreconstructed surface.[7,8] This dimer-like pairing model has been suggested as a preferred model, based on a comparison with angle-integrated photoemission data.[2] All of these models for Si(100)(2×1) produce metallic surface state bands, as does the ideal unreconstructed Si(100) surface geometry.

We have obtained new information about the surface state bands near the top of the valence bands using angle-resolved photoemission spectroscopy with the synchrotron radiation source at the University of Wisconsin-Madison. In particular, we have measured the surface density of states and one-electron surface band dispersions $E(k_{\parallel})$. Experimentally we find that the surface state bands are semiconducting, not metallic as previously believed, and observe energy band dispersions that disagree with all presently available model calculations.

A summary of our findings is presented in Fig. 2, where the surface state energy vs momentum band dispersion $E(\vec{k}_{\parallel})$ along the [010] crystal direction is shown (solid line), together with the "best" previous theoretical band dispersion due to Appelbaum and Hamann,[8] who "fit" previous photoemission and LEED results ($\vec{k}_{\parallel}$ is the electron wavevector parallel to the surface). In Fig. 2, E_F denotes the Fermi energy while the right side of the figure denotes the energy position of the underlying bulk Si band gap. It is seen in Fig. 2 that theory (dimer model[8]) predicted a metallic surface, with two surface state bands crossing E_F in the band gap above the valence band maximum. In contrast, experimentally we observe that the surface is semiconducting with a ~0.7eV gap between E_F and the surface state band which disperses from -0.7 eV at $\bar{\Gamma}$ = 0 to -1.1 eV at the surface Brillouin zone boundary [010]. Our results disagree qualitatively with all surface state dispersions calculated previously, i.e., the ideal surface, the vacancy model, the pairing model, and the zig-zag-chain model, and have stimulated new work on the Si(100) surface.

Experimental Energy vs. Momentum $E(\vec{k})$ Band Dispersions for Solids: GaAs. We have developed accurate new methods for directly determining the energy band dispersions $E(\vec{k})$ of a variety of materials—semiconductors, metals, metallic compounds, etc., using angle-resolved photoemission with synchrotron radiation. Such measurements are of fundamental interest in solid state physics because a knowledge of one-electron energy bands is central to understanding many physical and chemical properties of materials. As an example of our many studies, a brief description of our determination of the $E(\vec{k})$ dispersions of the prototype III-V semiconductor GaAs is given.

For semiconductors, despite numerous reported studies, only rather limited experimental information about band dispersions has been obtained previously. In particular, GaAs, being technologically important, has attracted much attention and is a model system for photoemission studies. We have determined the experimental band dispersions $E(\vec{k})$ of GaAs for the first time[13,14] along all three major symmetry directions Γ-Σ-X, Γ-Δ-X and Γ-Λ-L. Our accomplishments have been two-fold: (i) to give a relatively more complete one-electron description for GaAs from experimental measurements, and (ii) to illustrate the usefulness and success of such techniques which are of general utility for many materials.

Experimental band dispersions $E(\vec{k})$ for GaAs have been determined along ΓΣX, ΓΛL, and ΓΔX and are summarized in Fig. 3 (circles, squares, crosses, and diamonds). For comparison, we show calculated dispersions (dashed lines) based on a nonlocal pseudopotential model fit to optical and angle-integrated photoemission data. The theory agrees fairly well for GaAs (within ~0.4 eV, worst case), which is the best understood III-V semiconductor. In Fig. 3, $E(\vec{k})$ dispersions along ΓΣX (circles) were determined using normal emission from GaAs(110) with photon energies in the $25 \lesssim h\nu \lesssim 100$ eV range. The same GaAs(110)

surface was used to determine $E(\vec{k})$ dispersions along $\Gamma\Lambda L$ (diamonds), $\Gamma\Delta X$ (squares) and along $\Gamma\Sigma X$ (crosses) using angular- and $h\nu$-dependent angle-resolved photoemission techniques.[13,14] These techniques, which have been worked out for semiconductors for the first time, are of general utility and have been successfully applied to a number of selected materials (see Summary Section).

REFERENCES

1. D.E. Eastman, J.J. Donelon, N.C. Hien, and F.J. Himpsel, An Ellipsoidal Mirror Display Analyzer System for Electron Energy and Angular Measurements, J. Nucl. Instrum. Methods, 1980, (in press).

2. J.E. Rowe and H. Ibach, Phys. Rev. Lett. ***32***, 421 (1974).

3. F. Jona, H.D. Shih, A. Ignatiev, D.W. Jepsen, and P.M. Marcus, J. Phys. C***10***, L67 (1977).

4. M.J. Cardillo and G.F. Becker, Phys. Rev. Lett. ***40***, 1148 (1978).

5. R.E. Schlier and H.E. Farnsworth in Semiconductor Surface Physics (University of Pennsylvania Press, Philadelphia, 1957), pp. 3-22; J. Chem. Phys. ***30***, 917 (1959).

6. J.A. Appelbaum, G.A. Baraff, and D.R. Hamann, Phys. Rev. Lett. ***35***, 729 (1975).

7. G.P. Kerker, S.G. Louie, and M.L. Cohen, Phys. Rev. B***17***, 706 (1978).

8. J.A. Appelbaum, G.A. Baraff, and D.R. Hamann, Phys. Rev. B***15***, 706 (1978).

9. D.E. Eastman, F.J. Himpsel, J.A. Knapp, and K.C. Pandey, Proceedings of the 14th International Semiconductor Conference, Edinburgh, Scotland, September 1978.

10. T.D. Poppendick, T.C. Ngoc, and M.B. Webb, Surf. Sci. ***75***, 287 (1978).

11. J.A. Appelbaum and D.R. Hamann, Surf. Sci. ***74***, 21 (1978).

12. S.Y. Tong and A.L. Maldonado, Surf. Sci. ***78***, 459 (1978); M.A. Van Hove and K.A.R. Mitchell, Surf. Sci. (in press).

13. T.-C. Chiang, J.A. Knapp, and D.E. Eastman, Sol. St. Commun. ***31***, 917 (1979).

14. T.-C. Chiang and D.E. Eastman, Angle-Resolved Photoemission, Valence Band Dispersions $E(\vec{k})$, and Electron and Hole Lifetimes for GaAs, Phys. Rev. B, 1980 (in press).

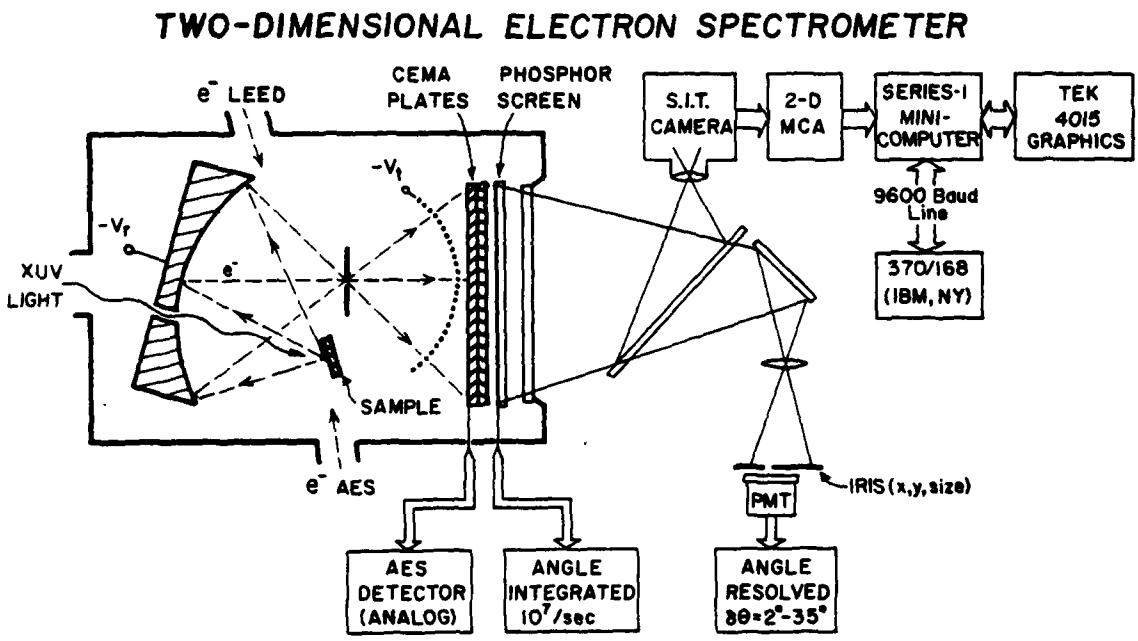

Figure 1 Schematic diagram (top view) of two-dimensional electron spectrometer system. The retarding field ellipsoidal low pass filter, retarding field spherical grid high pass filter, and an area detector which consists of a CEMA multiplier and phosphor screen are shown. Several detectors for angle-resolved PES, angle-integrated PES and Auger measurements are schematically shown, including a data acquisition system for recording digitally the entire screen.

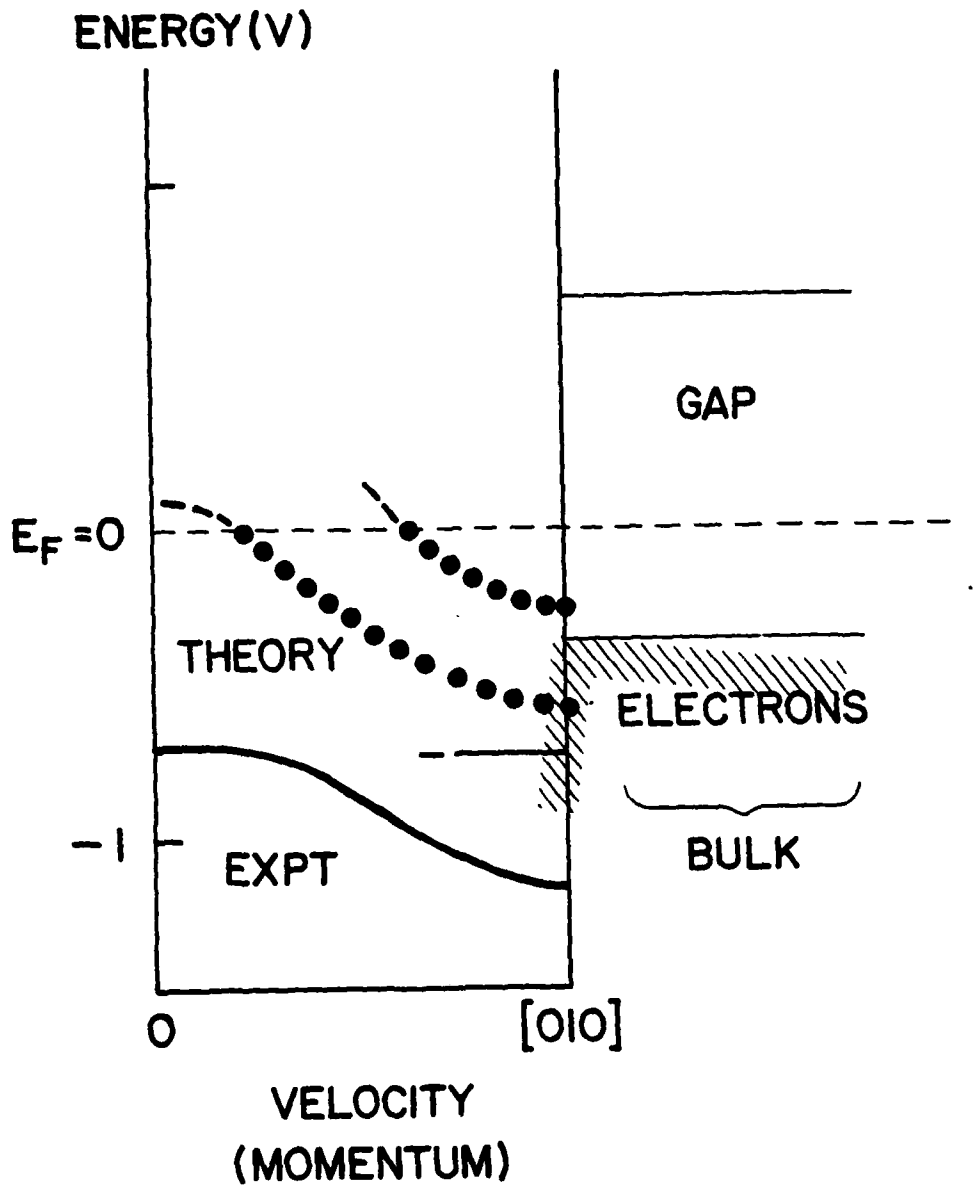

Figure 2 Energy band dispersion for surface states on Si(100)-(2×1) surface. The theory curves (dotted) (Ref. 8) correspond to a metallic surface with surface states in the fundamental gap while we have experimentally determined that there are lower-lying surface states with a semiconducting surface.

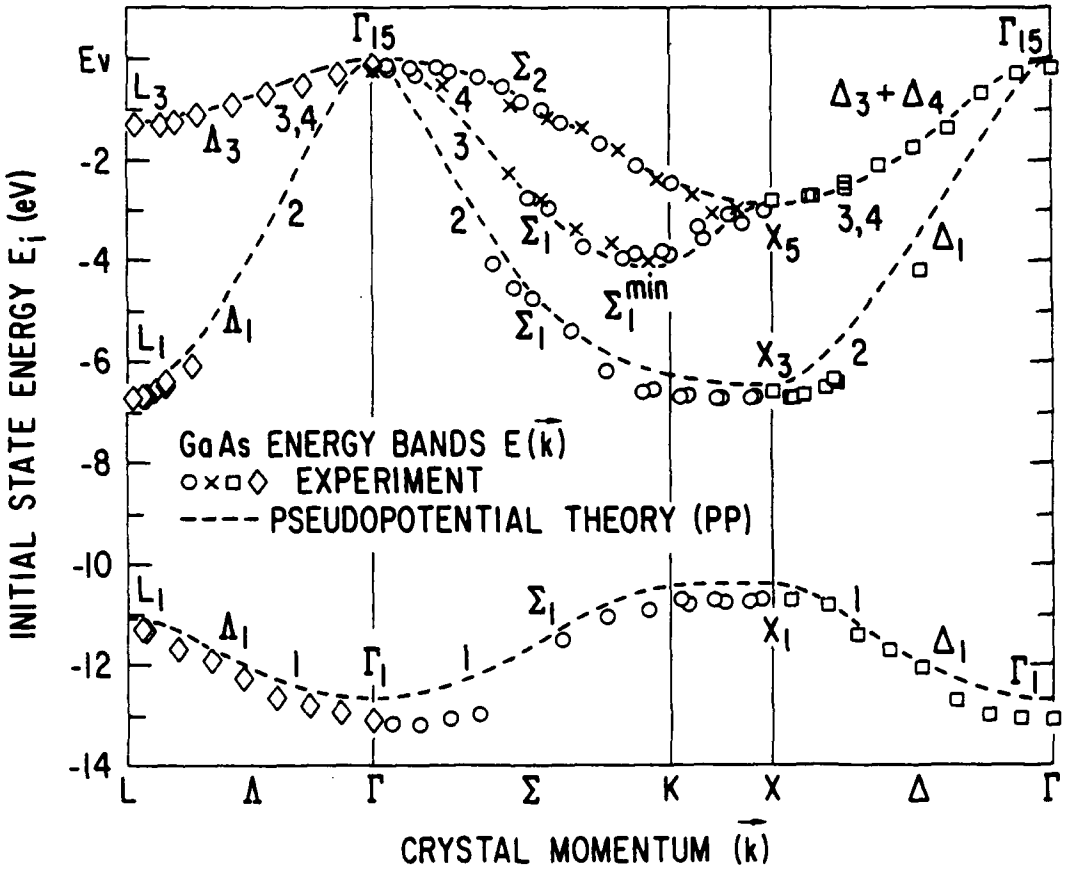

Figure 3 Experimental energy band dispersion $E(\vec{k})$ along the three main symmetry directions for GaAs (circles, crosses, diamonds, squares; see text). The dashed line depicts a theoretical calculation by Pandey and Phillips using a nonlocal pseudopotential which was fit to optical and photoemission data.

II. SUMMARY OF WORK COMPLETED UNDER CONTRACT

In the following, a brief summary is given of published research papers that were supported in part by the Air Force Office of Scientific Research under contract F446720-70-C-0089. For clarity, these research papers (34 in all) have been grouped into five sub-areas of research:

A. Electronic structure of semiconductor surfaces and interfaces.
B. Electronic structure of group IV and group III-V semiconductors.
C. Electronic structure of metal surfaces.
D. Electronic structure of metals and metallic compounds.
E. Studies of electronic many-electron effects.

A. Electronic Structure of Semiconductor Surfaces and Interfaces.

1. Empty surface states on semiconductors: Their interactions with metal overlayers and their relation to Schottky barriers.

   Measurements we have made of $(E_F\text{-}E_v)_{surface}$ for n-type GaAs (110) indicate that, contrary to some previous publications, there are no unoccupied surface states in the band gap of GaAs(110), i.e., $(E_F\text{-}E_v)_{surface}$ is equal to the band gap. This result has two major implications: (1) $(E_F\text{-}E_v)_{surface}$ is exceedingly sensitive to the quality of the cleavage, as well as to low exposures ($<$1L) of residual gases in UHV systems (even though gas sticking probabilities appear to be low); thus considerable care must be executed in using band bending measurements as a probe of surface states. (2) Partial yield and electron-energy-loss measurements show transitions from core levels to unoccupied surface states at energies that, in the absence of excitonic shifts, would place the one-electron energy of these unoccupied surface states on GaAs(110) ~ 0.5 eV below this observed position of E_F. One must therefore conclude that these transitions involve strong excitonic binding, with an exciton binding energy $E_{Ex} \gtrsim 0.6$ eV for GaAs(110). (W. Gudat, D. E. Eastman, and J. L. Freeouf, J. Vac. Sci. Technol. *13*, 250 (1976).)

2. Electronic surface properties of III-V semiconductors: Excitonic effects, band-bending effects, and interactions with Au and O adsorbate layers.

   Photoemission studies of valence bands, core levels, empty surface states, and band bending for cleaved GaAs (110) are described. These studies show that there are no intrinsic band-gap surface states for GaAs (110), and that large ($\gtrsim$ 0.5 eV) excitonic binding energies are involved in core-level-to-empty-surface-state transitions (e.g., using yield spectroscopy or electron energy-loss spectroscopy). Studies of the effects on chemisorbed oxygen and thin Au overlayers on InAs (110) and GaAs (110) surfaces are also described. Trends and correlations in III-V semiconductor empty surface states are discussed. (W. Gudat and D. E. Eastman, J. Vac. Sci. Technol. 13, 831 (1976).)

3. Photoemission and band structure studies of the GaAs(110) Surface.

   We have studied the electronic and geometrical structure of the cleaved GaAs(110) surface, using experimental ultraviolet photoemission spectroscopy

(UPS) of both filled and empty surface states together with tight-binding calculations. We have considered several different types of structural models, including the relaxation model in which surface Ga atoms move into, and As atoms move out of, the surface by an amount such that the plane through the nearest neighbor Ga and As atoms makes a tilt angle, θ_T , with the corresponding plane in the ideal surface while bond lengths remain constant. We show that this model with a tilt angle $\theta_T \sim 19°$ — in contrast with $\theta_T \sim 35°$ as previously concluded from a LEED (low energy electron diffraction) analysis — adequately accounts for the photoemission spectroscopy data. A description of the nature of surface states including the local s- and p-orbital densities of states and dispersion relations is given for this relaxation model. (K. C. Pandey, J. L. Freeouf, and D. E. Eastman, J. Vac. Sci. Technol. ***14***, 904 (1977).)

4. Chemisorption of chlorine on Si(111) 7×7 and 1×1 surfaces.

Using ultraviolet photoemission spectroscopy (UPS) in conjunction with theoretical calculations, we have studied the reaction of gaseous chlorine with Si(111) 7×7 and 1×1 surfaces. The UPS spectra of the two chlorine saturated surfaces are very similar and consist of four peaks, a sharp main peak at −10.7 eV and smaller ones at −7.5, −13.0, and −15.7 eV relative to the vacuum level. Both the peak positions and their relative intensities are in quantitative agreement with a theoretical calculation for a structural model in which a single chlorine atom sits on top of each surface Si atom, indicating that Cl_2 decomposes at the surface to make strong covalent bonds with Si. (K.C. Pandey, T. Sakurai, and H.D. Hagstrom, Phys. Rev. B***16***, 3648 (1977).)

5. Reaction of atomic hydrogen with Si(111) surfaces: formation of monohydride and trihydride phases.

By using a realistic tight-binding or LCAO (linear combination of atomic orbitals) model, detailed calculations of surface states, local densities of states, and theoretically simulated photoemission spectra have been carried out for two qualitatively distinct structural models for chemisorption of atomic hydrogen on Si(111)1×1 surfaces. In the low-coverage model, called the monohydride phase or Si(111):H, it is assumed that a single hydrogen atom sits on top of each surface Si atom, thus saturating all dangling bonds. In the high-coverage model, designated as the trihydride phase or Si(111):SiH_3, SiH_3 radicals are bonded to the surface Si atoms. Due to the radically different atomic structures, the theoretical spectra of the two phases show striking differences. A comparison of the theoretical spectra with the ultraviolet photoemission spectra taken during hydrogen chemisorption on the quenched Si(111)1×1 surface clearly shows that at low coverages the monohydride is formed, while at high coverages the trihydride phase is formed. Formation of the monohydride phase is expected on simple chemical and structural considerations, and it has been observed on other Si surfaces. However, formation of the trihydride phase is unique to Si(111)1×1 and as such, it has important implications regarding the structure and stability of clean Si(111)1×1. (K. C. Pandey, IBM Journal of Research and Development, ***22***, 250 (1978).)

6. Atomic and electronic structure of semiconductor surfaces

The electronic structure of surfaces, which can be determined by various electron/ion spectroscopies including ultraviolet photoemission spectroscopy

(UPS), is dependent on the surface atomic geometry. Thus, it is possible to determine the surface atomic structure via structure-dependent theoretical analyses of these experimental spectra. Because of the complexity of such systems, a simple but accurate theoretical scheme is required. We show that the valence electronic states and atomic structures of semiconductor surfaces—both clean and with chemisorbed species as well as relaxed and/or reconstructed—can be determined using a tight-binding model. Such calculations together with UPS data show that the annealed Si(111)7×7 surface contains about 25% vacancies. For GaAs(110), we have found that the Ga atoms move into, and As atoms move out of the surface with small bond length distortions so that a plane through them makes an angle of about 20° with the surface. We show that H chemisorbed on Si(111) has two distinct structural phases: a monohydride phase at low coverages, and a rather unexpected trihydride phase at high coverages. (K. C. Pandey, ***Physics of Semiconductors***, 1978, Inst. of Phys. Conf. Series 43, Bristol and London, 1051 (1979)).

7. Atomic and electronic structure of Si(111)7×7 surface.

Calculations of the surface electronic structure of the Si(111)7×7 surface for several different structural models have been carried out. Two structural models, a vacancy model and a buckled surface model, give surface electronic structures consistent with angle-averaged photoemission spectra. However, the origin and symmetry of surface states in the two models are different. We point out that these differences, in conjunction with further experiments, can be used to decide between the two models. (K. C. Pandey, *Physics of Semiconductors 1978*, Inst. of Phys. Conf. Series 43, Bristol and London, 1051 (1979).)

8. Surface electronic structure studies of GaAs(110).

Angle-resolved photoemission using synchrotron radiation from GaAs(110) has been studied in conjunction with tight binding calculations of the surface electronic structure. Emission from two new surface resonances—which were predicted to exist only for a relaxed surface—have been identified near the edges of the surface Brillouin zone at $\bar{X}$ and $\bar{X}'$. Also, measurements of the dispersion of the As-derived surface state near the valence band maximum, first reported elsewhere, have been extended from $\bar{\Gamma}$ to the zone edge $\bar{X}$ and a band width of 0.6 eV has been determined. All of these observations, including those reported elsewhere of intrinsic surface states on GaAs(110) are accounted for by a tight binding model calculation for a relaxed surface (~ 19° bond angle rotation). (J. A. Knapp, D. E. Eastman, K. C. Pandey, and F. Patella, J. Vac. Sci. Technol. *15*, 1252 (1978).)

9. Angle-resolved photoemission studies of semiconductor bulk and surface states.

Polarization-dependent angle-resolved photoemission studies using synchrotron radiation together with theoretical models permit both energy and momentum information (e.g., E ($\hat{k}$) dispersions) to be obtained for semiconductor bulk and surface states. Illustrative applications for intrinsic surface states (Si(111)-(7×7)), adsorbate states (Si(111):H), and bulk electronic states (GaAs(110)) are described. (D. E. Eastman, F. J. Himpsel, J. A. Knapp and K. C. Pandey, ***Physics of Semiconductors 1978***, Inst. of Phys. Conf. Series 43, Bristol and London, 1059 (1979).)

10. Quantum photoyield of diamond(111) — a stable negative affinity emitter.

Quantum photoyield and secondary electron distributions have been measured for an unreconstructed diamond(111) surface (type IIb, gem quality blue-white semiconductor). This chemically inert surface exhibits a negative electron affinity, resulting in a stable quantum yield that increases linearly from photothreshold (5.5 eV) to ~ 20% at 9 eV, with a very large yield of ~ 40-70% for $13 \lesssim h_\nu \lesssim 35$ eV. For all photo energies, secondary electron energy distributions show a dominant ~ 0.5 eV wide emission peak at the conduction band minimum (Δ_1^{min}=5.50±0.05 eV above the valence band maximum Γ_{25}'). In contrast with recent self-consistent calculations (J. Ihm, S.G. Louie, and M.L. Cohen, Phys. Rev. B*17*, 769 (1978)), no occupied intrinsic surface states with ionization energies in the fundamental gap (the Fermi level was 1 eV above Γ_{25}') were observed. Likewise, the measured photothreshold ($E_{Vac}-\Gamma_{25}'$) is significantly smaller than calculated (7.0±0.7 eV). (F. J. Himpsel, J. A. Knapp, J. A. VanVechten and D. E. Eastman, Phys. Rev. B*20*, 624 (1979).)

11. Photoemission studies of intrinsic surface states on Si(100).

We have determined the energy vs $k_\parallel$ dispersion of intrinsic surface states on Si(100) (2×1) by means of angle-resolved photoemission with synchrotron radiation. For $k_\parallel$=0, there is a very pronounced surface state 0.7 eV below E_F(i.e., ~ 0.4 eV below the top of the valence band) which disperses downwards with increasing $k_\parallel$. At J′ on the boundary of the surface Brillouin zone, we find two states with binding energies of 0.7 and 1.2 eV with respect to E_F. A number of geometrical models and their corresponding theoretical surface state bands have recently been published for Si(100)(2×1). Our results disagree qualitatively with all surface state dispersions calculated to date, i.e., the ideal surface, the vacancy model, the pairing model, and the zig-zag-chain model. Namely, we observed semiconducting surface state bands with a low state density at E_F while all models calculated to date yield metallic surface states with a large state density at E_F. (F. J. Himpsel and D. E. Eastman, J. Vac. Soc. Technol. *16*, 1297 (1979).)

12. Microscopic compound formation at the Pd-Si(111) interface.

Photoemission studies of Pd on clean Si(111) surfaces show that formation of the Pd_2Si compound dominates the microscopic chemistry and properties of the Pd-Si interface. No evidence is found for interface dipoles or occupied metal-induced interface states in this system. The Pd_2Si reaction product (a metal) has an electronic structure more like that of the noble metals than the transition metals, with an occupied 4d band located ~ 2.75 eV below the Fermi energy. (J.L. Freeouf, G.W. Rubloff, P.S. Ho, and T.S. Kuan, Phys. Rev. Lett. *43*, 1836 (1979).)

13. Silicide Schottky barriers: an elemental description.

A model for reactive Schottky barrier formation has been proposed and applied to silicide contacts on silicon. Approximate workfunctions calculated assuming a silicon excess near the silicide/silicon interface reconcile measured barrier heights with a simple Schottky description of their energetics. (J.L. Freeouf, Sol. St. Commun. *33*, 1059 (1980).)

14. Geometrical and electronic structure of Si(001) and Si(111) surfaces: a status report.

A critical review of recent studies of the geometrical and electronic structure of the Si(001) and Si(111) surfaces has been made. Emphasis is placed on low-energy electron diffraction (LEED) studies of the geometrical structure, photoelectron spectroscopy studies of the electronic structure, and theoretical studies of the electronic and geometric structure of the Si(111)-(2×1), Si(111)-(7×7), Si(111)-(1×1), and Si(001)-(2×1) surfaces. (D.E. Eastman, J. Vac. Sci. Technol. (in press).)

B. Electronic Structure of Group IV And Group III-V Semiconductors

15. Photoemission spectroscopy using synchrotron radiation. II. The electronic structure of germanium.

We analyze photoemission spectra for Ge obtained for photon energies $6.5 \leq h\nu \leq 25$ eV and determine the position of energy bands at symmetry points for both filled and empty bands within 1 Ry of the gap. This experimental band structure is obtained using a recently developed anisotropic direct-transition model of photoemission applicable to cleaved single-crystal semiconductors. For the band-structure determination we also employ a direct transition analysis of optical spectra obtained by others. We fit nonlocal-pseudopotential calculations to the experimentally-determined band positions, and thereby determine the importance of both energy and $\ell = 2$, angular momentum nonlocality in the pseudopotential. Our results for the position of high-lying conduction-band states suggest 0 to + 10% self-energy (exchange-correlation) corrections to the energy of electrons excited into the conduction bands. Energy bands which provide a good fit to the experimental band positions are used, along with pseudo-wave-function matrix elements, to calculate various physical properties (photoemission spectra, optical-response functions, and one-electron state densities), and the results of these calculations are compared with experiment. The quality of the fits obtained indicates that the electronic excited-state (and ground-state) properties of Ge for excitations far from the gap are described well by a one-electron model. (W. D. Grobman, D. E. Eastman, and J. L. Freeouf, Phys. Rev. B*12*, 4405 (1975).)

16. Angle-resolved photoemission and valence band dispersions $E(\vec{k})$ for GaAs: Direct vs. Indirect Models.

Angle-resolved photoemission measurements for GaAs(110) have been extended to $h\nu$=100 eV. These results show that dominant emission peaks are due to direct transitions. Weaker one-dimensional density of states features sometimes observed are due to surface umklapp/secondary cone and lifetime effects. Accurate band dispersions $E(\vec{k})$ for all four valence bands of GaAs along the [110] direction are given using simple normal emission and off-normal emission methods. Electron and hole lifetimes are directly determined. (T.-Chiang, J.A. Knapp, and D.E. Eastman, Sol. St. Commun. *31*, 917 (1979).

17. Angle-resolved photoemission and valence band dispersions $E(\vec{k})$ and electron and hole lifetimes for GaAs.

Accurate valence band dispersions $E(\vec{k})$ along the major symmetry directions Γ-Σ-X, Γ-Λ-X, nd Γ-Δ-L have been determined for GaAs using simple angle-

resolved photoemission techniques of general utility with synchrotron radiation for $25 \leq h\nu \leq 100$ eV. At these photon energies, emission features can be understood within the direct transition model and spectral peaks can be classified roughly into two categories: one being those associated with primary cone emission with a lifetime broadened free-electron-like final state dispersion, and the other (usually weaker) being those associated with secondary cone/surface umklapp emission which emphasizes valence band critical points with high state densities. Valence band dispersions $E(\vec{k})$ along the Γ-K-X symmetry line perpendicular to the surface are determined using normal emission spectra (primary cone peaks) from the (110) surface at various photon energies. Valence band dispersions $E(\vec{k})$ along Γ-K-X, Γ-Δ-X, and Γ-Λ-L symmetry lines parallel to the surface are determined using off-normal emission spectra (primary cone peaks) from the same (110) surface with fixed perpendicular component of the electron momentum $\hbar k_\perp$ at the zone center (extended zone scheme) and varying parallel component of the electron momentum $\hbar k_\parallel$, which are obtained by suitably varying $h\nu$ and emission angles. Experimental valence band dispersions and critical points are compared with other theoretical and experimental results. Simple formulae are derived to relate the widths of spectral peaks to electron and hole lifetimes. Initial hole lifetimes at valence critical points and typical final electron lifetimes are obtained. The latter yields final state momentum broadening (typically $\lesssim$ 10% of the Brillouin zone size) which are consistent with the direct transition model. (T.-C. Chiang and D.E. Eastman, Phys. Rev. (in press).)

18. Experimental energy band dispersions, critical points, and spin-orbit splittings for GaSb using angle-resolved photoemission.

We have determined energy band dispersions $E(\vec{k})$ and critical points for GaSb using angle-resolved photoemission techniques. With a normal emission configuration and photon energies between 24 and 95 eV, the valence band dispersions $E(\vec{k})$ have been obtained along the Γ-K-X direction, with the spin-orbit splitting $\Delta_0(\Gamma_8\text{-}\Gamma_7)$ clearly observed. With an off-normal emission configuration, we have also determined the valence band critical point energies at the L point, with the spin-orbit splitting $\Delta_1(L_{4,5}\text{-}L_6)$ clearly observed. Experimental valence band critical point energies at Γ, X and L are compared with recent theoretical results. Using published transition energies determined from reflectance measurements, we have also obtained the low-lying conduction band critical point energies. These valence and conduction band critical point energies are tabulated to facilitate comparisons with other experimental and theoretical results. (T.-C. Chiang and D.E. Eastman, Phys. Rev. (in press).)

C. Electronic Structure of Metal Surfaces.

19. Observation of a Λ_1-Symmetry Surface State on Ni(111).

An s-p-like intrinsic surface state on Ni(111) has been found which has an energy of $E_i = -0.25$ eV relative to the Fermi energy at $\bar{\Gamma}$ and lies between the L_3 ($E_i \simeq -0.15$ eV and L_2' ($E_i = -0.9$ eV) bulk states. Its momentum dispersion (E vs $\vec{k}_\parallel$) and $h\nu$-dependent photoionization cross section have been

determined using angle-resolved photoemission with synchrotron radiation. The existence of this state significantly affects spin-polarized photoemission, chemisorption, band-structure, and exchange-splitting interpretations for Ni. (F.J. Himpsel and D.E. Eastman, Phys. Rev. Lett. ***41***, 507 (1978).)

20. Intrinsic Λ_1-symmetry surface state on Co(0001).

An intrinsic surface state on Co(0001) has been found using angle-resolved photoemission with synchrotron radiation which has an energy of E_i= -0.3 eV at $\bar{\Gamma}$ (zone center) relative to the Fermi energy E_F . Its symmetry has been determined to be of Λ_1 character using measurements with s- and p-polarized radiation. Its momentum dispersion (E vs $\vec{k}_{\parallel}$) and $h\nu$-dependent photoionization cross section have also been determined. At the zone center $\bar{\Gamma}$, the surface state lies in an absolute energy gap just above the uppermost $\Lambda_{3\uparrow}$ d-like (E_i = -0.35 eV) bulk state, well above the uppermost sp-like, Λ_1 state (E_i= -1.15 eV), and below occupied $\Lambda_{3\downarrow}$ d-like bulk states near Γ (energies between E_i = -0.05 eV and 0). As previously reported for Ni, this surface state is extremely sensitive to absorbates and significantly affects field emission, spin-polarized photoemission, chemisorption, etc. for Co(0001). (F.J. Himpsel and D.E. Eastman, Phys. Rev. B***20***, 3217 (1979).)

D. Electronic Structure of Metals and Metallic Compounds.

21. Electronic structure of the thorium hydrides ThH_2 and Th_4H_{15}.

Photoelectron spectroscopy using synchrotron radiation has been used to study the electronic structure of single-phase stoichiometric ThH_2 and Th_4H_{15}. Th-derived conduction bands are observed together with lower-lying hybridized bonding bands. For Th_4H_{15}, a narrow d-like conduction band (~ 0.6-eV full width at half-maximum) separated from other bands by a 2-eV band gap is seen. Energy-dependent cross-section measurements for the various bands have been used to determine hybridization and angular momentum character. (J.H. Weaver, J.A. Knapp, D.E. Eastman, D.T. Peterson, and C.B. Satterwaite, Phys. Rev. Lett. ***39***, 639 (1977).)

22. Experimental band structure and temperature-dependent magnetic exchange splitting of nickel using angle-resolved photoemission.

Using angle-resolved photoemission and synchrotron radiation, we have determined the energy-versus-momentum valence-band dispersion relations for a Ni(111) crystal. The temperature-dependent ferromagnetic exchange splitting has been directly observed. Both the d-band width (~3.4 eV at L) and exchange splitting (0.31 eV) are much smaller than theoretical estimates (~4.5 eV wide at L with ~0.7-eV splitting, respectively, at 293 K. (D.E. Eastman and F.J. Himpsel, Phys. Rev. Lett. ***40***, 1514 (1978).)

23. Direct determination of lifetime and energy dispersion for the empty Δ_1 conduction band of copper.

We present an accurate determination of the energy dispersion (E vs k) and the first direct determination of the energy-dependent lifetime $\Gamma(E)$ of well-defined excited Bloch states in a crystal. Using angle-resolved photoemission for Cu(100), we find that the lifetime broadening increases from Γ = 1.2 eV (6×10^{-16} sec) for Δ_1 conduction-band states ranging 10.5 to 13.5 eV above

the Fermi level. The measured dispersion (~2% accuracy) shows a reduced effective mass (m/m_0=0.90—0.94) which is related to self-energy effects. (D.E. Eastman, J.A. Knapp, and F.J. Himpsel, Phys. Rev. Lett. ***41***, 825 (1978).)

24. Experimental energy dispersions for valence and conduction bands of palladium.

Using angle-resolved photoemission with synchrotron radiation, we have determined accurate energy-versus-momentum dispersion relations along the <111> direction using a Pd(111) crystal. The energy E ($\lesssim$ 0.1 eV accuracy) and the momentum parallel to the surface $\vec{k}_\parallel$ are measured directly. The perpendicular component of the momentum $k_\perp$ is obtained from the measured final energy via a calculated free-electron-like final band that is found to be accurate within ±5% of the zone-boundary momentum by comparison with certain critical points that have been measured directly (L_1, Γ'_2, and Γ_{15}). For the initial bands, we find the dispersions of the two d-like Λ_3 bands and of the sp-type Λ_1 band. Measured critical points (in eV) for bands numbered with increasing energy are: $\Gamma_{2,3,4}$ = -2.55 ± 0.15, $\Gamma_{5,6}$ = -1.15 ± 0.1, Γ_7 = 18.4 ± 0.5, Γ_8 = 21.7 ± 0.5, L_4 = -0.4 ± 0.2, L_5 -0.1 ± 0.1, and L_7 = 7.7 ± 0.3. Spin-orbit splitting (~0.4 eV maximum) is observed for the upper Λ_3 band. (F.J. Himpsel and D.E. Eastman, Phys. Rev. B***18***, 5236 (1978).)

25. Experimental energy-band dispersions and exchange splitting for Ni.

Angle-resolved polarization-dependent photoelectron spectroscopy using synchrotron radiation has been used to determine the energy-versus-momentum band dispersions and magnetic exchange splitting of Ni. Using Ni(111) and Ni(100) crystals, the band dispersions along the Γ-L and Γ-X lines have been determined for the s and d bands. The temperature-dependent magnetic exchange splitting ΔE_{ex} of the upper Λ_3 band has been directly observed and found to be independent of momentum $\vec{k}$ for a large region of the Brillouin zone. The experimental value of ΔE_{ex} = 0.31 ± 0.03 eV is smaller than recent calculated values ($0.6 \lesssim \Delta E_{ex} \lesssim 0.9$ eV) obtained with spin-polarized self-consistent band calculations. Also, calculated d-band widths are larger (typically 40%) than measured (3.4 eV at L). Our results are consistent with Fermi-surface data and the polarization reversal observed in spin-polarized photoemission. A number of previous contradictory photoemission studies of Ni are discussed in view of our results. The observed bands show that ferromagnetic nickel can be described by a Stoner-Wohlfarth-Slater spin-split band model. (F.J. Himpsel, J.A. Knapp, and D.E. Eastman, Phys. Rev. B***19***, 2919 (1979).)

26. Experimental energy band dispersions and lifetimes for valence and conduction bands of copper using angle-resolved photoemission.

Energy band dispersions and electron lifetimes have been determined for both valence and conduction band states of copper using angle-resolved photoemission with polarized synchrotron radiation in the $5 \lesssim h\nu \lesssim 35$ eV photon energy range. Dispersion relations for the occupied s-p and 3d bands of Cu along the Γ-X and Γ-L symmetry lines (including critical points at Γ, X, and L) have been determined with an accuracy of 0.05-0.1 eV and $\lesssim$ 5% of the zone boundary momentum. Band symmetries have been deduced using polarization selection rules. The dispersion relation has also been accurately determined for the unoccupied Δ_1 conduction band along Γ-X at ~10-15 eV above

the Fermi energy E_F ; this band has a reduced effective mass ($m \simeq .90$-$.94$) which is related to self-energy effects. Lifetimes have been directly measured for excited hole states (the lifetime broadening Γ_h increases from ~0.2 to 0.5 eV FWHM for d-band energies from 2 to 5 eV below E_F) as well as for excited electron states in the Δ_1 conduction band ($\Gamma_e \simeq 1.0$ to 2.0 eV for energies 10 to 15 eV above E_F). The energy dispersion and $h\nu$-dependent photoionization cross section of the s-p surface state on Cu(111) are reported. Previous theoretical and experimental studies of copper are compared with our accurate E vs. $\vec{k}$ dispersions. (J.A. Knapp, F.J. Himpsel, and D.E. Eastman, Phys. Rev. B*19*, 4952 (1979).)

27. Temperature dependence of bulk and surface energy bands in copper using angle-resolved photoemission.

We have directly measured thermally induced changes in surface and bulk energy-band dispersions of copper by examining angle-resolved photoemission from Cu(111) and Cu(100) surfaces for temperatures from 25 to 500°C. Polarized synchrotron radiation was used as the photon source. Observed shifts in the bulk band structure are in reasonable agreement with energy shifts calculated for the corresponding temperature-dependent lattice changes. The measured temperature coefficient for the upper d band along Λ is $1.5(\pm 0.1) \times 10^{-4}$ eV/K, while the lower edge of the d bands shifts by $2.0(\pm 0.2) \times 10^{-4}$ eV/K. The d-band width decreases with temperature at a rate of $0.5(\pm 0.2) \times 10^{-4}$ eV/K as it shifts to higher energy. The Cu(111) surface state shifts toward E_F with a measured temperature coefficient of $2.7(\pm 0.1) \times 10^{-4}$ eV/K. (J.A. Knapp, F.J. Himpsel, A.R. Williams, and D.E. Eastman, Phys. Rev. B*19*, 2844 (1979).)

28. Symmetry method for the absolute determination of energy-band dispersions $E(\vec{k})$ using angle-resolved photoelectron spectroscopy.

Angle-resolved spectra for emission in a mirror plane as a function of emission ang. : and photon energy $h\nu$ show critical-point behavior in interband intensities for transitions on zone boundaries. For such transitions, the absolute energies E and crystal momentum $\vec{k}$ for both the initial and final states are given by $h\nu$ and the emission angle. $E(\vec{k})$ dispersions have been determined for several d bands and conduction bands along the Δ, Λ, and ε axes of copper. (Eberhard Dietz and D.E. Eastman, Phys. Rev. Lett *41*, 1674 (1978).)

29. Experimental band dispersions $E(\vec{k})$ along three main symmetry lines of LaB_6 using angle-resolved photoemission from one crystal surface.

Accurate valence band dispersions $E(\vec{k})$ of LaB_6 have been determined along three main symmetry lines ΓM, ΓX, and XM using one single crystal (001) surface by a simple new photoemission technique of general utility. Using direct interband transitions, $E(\vec{k})$ dispersions are mapped out by suitably scanning polar emission angle and the photon energy. Detailed results agree well with recent Xα-APW energy band calculations. (M. Aono, T.-C. Chiang, J.A. Knapp, T. Tanaka, and D.E. Eastman, Sol. St. Commun. *32*, 271 (1979).)

30. Experimental exchange-split energy band dispersions for Fe and Co.

Using angle-resolved photoemission with single crystal Fe(111) and Co(0001) we have determined accurate exchange-split energy band dispersions $E(\vec{k})$ along symmetry lines. For Fe, Co, and Ni, respectively, occupied d-band widths are 3.1 eV (P), 3.8 eV (L) and 3.4 eV (L,X) while exchange splittings are ~1.5 eV (P), ~1.1 eV (Γ) and 0.3 eV (near L). Comparison with theory shows that state-of-the-art ab-initio calculations describe the strong ferromagnets Fe and Co much better than Ni. (D.E. Eastman, F.J. Himpsel and J.A. Knapp, Phys. Rev. Lett. ***44***, 95 (1980).)

31. Experimental energy band dispersions and magnetic exchange splitting for cobalt.

We have determined E vs. $\vec{k}$ energy band dispersions of cobalt for s- and d-bands along the hexagonal axis $\Gamma\Delta A$ ([0001]-direction) via angle resolved photoelectron spectroscopy from a Co(0001)-face using synchrotron radiation. We obtain the magnetic exchange splitting at Γ for the upper d-band (0.85 ± 0.2 eV) and lower d-band (1.2 ± 0.3 eV). The overall occupied d-band width (~3.8 eV at L) is about 20% narrower than a state-of-the-art self-consistent band calculation using a local density theory of exchange-correlation. The top of the majority spin d-bands is 0.35 eV below E_F. There is a small Γ-centered minority electron pocket at E_F which explains previously unidentified deHaas van Alphen orbits. We present dipole selection rules for the Δ axis of a hcp lattice and show that the number of allowed transitions is reduced drastically for emission along the Δ-axis. The allowed transitions can be interpreted in the same way as those for emission normal to a (111) face of a fcc lattice. (F.J. Himpsel and D.E. Eastman, Phys. Rev. (in press).)

E. Studies of Electronic Many-Electron Effects..

32. Resonant photoemission shake-up and Auger processes at the 3p photothreshold in Ga and GaP.

Resonant photoemission $3d^8$ shake-up satellites in Ga metal and GaP, which are closely related to $M_{2,3}M_{4,5}M_{4,5}$ Auger transitions, have been observed at the 3p photothreshold of Ga. By analyzing the line positions, multiplet structure, and resonant behavior near threshold, we have determined the excitonic binding energies and correlation energies for various one-hole and two-hole excited states. While these two-hole excitations in Ga metal and GaP are similar because of their quasi-atomic nature, important differences are observed which are due to different final state screening mechanisms for a metal and an insulator. The present results are compared with those for Cu and Ni. (T.-C. Chiang and D.E. Eastman, Phys. Rev. (in press).

33. Observation of the transition from the adiabatic to the sudden regime for the $M_3M_{4,5}M_{4,5}(^1G)$ Auger excitation in zinc.

We have observed that the photoexcited $M_3M_{4,5}M_{4,5}$ (^1G) Auger line in Zn asymmetrically broadens to lower energy with increasing photon energy. The broadening can be described by a change in the asymmetry parameter $\Delta\alpha=0.09$ using a Doniach-Sunjic lineshape. This is the first evidence for the

transition from the adiabatic to the sudden regime in a solid. The onset of this change ~ 14 eV above threshold is related to 3d screening electron excitations which are seen as 3p core level satellites. (F.J. Himpsel, D.E. Eastman, and E.E. Koch, Phys. Rev. Lett. *44*, 214 (1980).)

34. Two-electron resonances at the 3p-threshold of Cu and Ni.

A sharp 3d-electron satellite excitation has been found for Cu which exhibits a strong resonant enhancement (~×5) at the Cu 3p core level threshold similar to the 6 eV resonant satellite observed previously in Ni. This satellite, which has two peaks at 11.8 and 14.6 eV below E_F, is identified as a quasi-atomic two-electron excitation with two 3d-holes plus one 4s electron ($3d^8 4s$). Present models for the Ni resonant satellite are not able to describe our Cu results. (M. Iwan, F.J. Himpsel, and D.E. Eastman, Phys. Rev. Lett. *43*, 1829 (1979).)

III. LIST OF PUBLICATIONS UNDER CONTRACT

A. Electronic structure of semiconductor surfaces and interfaces.

1. Empty Surface States on Semiconductors: Their Interactions with Metal Overlayers and Their Relation to Schottky Barriers, W. Gadat, D.E. Eastman and J.L. Freeouf, J. Vac. Sci. Technol. ***13,*** 250 (1976).

2. Electronic Surface Properties of III-V Semiconductors: Excitonic Effects, Band Bending Effects, and Interactions with Au and O Adsorbate Layers, W. Gudat and D.E. Eastman, J. Vac. Sci. Technol ***13,*** 831 (1976).

3. Photoemission and Band-Structure Studies of the GaAs(110) Surface, K.C. Pandey, J.L. Freeouf and D.E. Eastman, J. Vac. Sci. Technol. ***14,*** 904 (1977).

4. Chemisorption of Chlorine on Si(111) 7×7 and 1×1 Surfaces, K.C. Pandey, T. Sakurai, and H.D. Hagstrom, Phys. Rev. B***16,*** 3648 (1977).

5. Reaction of Atomic Hydrogen with Si(111) Surfaces: Formation of Monohydride and Trihydride Phases, K.C. Pandey, IBM J. Res. Develop. ***22,*** 250 (1977).

6. Atomic and Electronic Structure of Semiconductor Surfaces, K.C. Pandey, J. Vac. Sci. Technol. ***15,*** 440 (1978).

7. Atomic and Electronic Structure of Si(111)7×7 Surface, K.C. Pandey, ***Physics of Semiconductors 1978*** Inst. of Phys. Conf. Series 43, Bristol and London, 1051 (1979).

8. Surface Electronic Structure Studies of GaAs(110), J.A. Knapp, D.E. Eastman, K.C. Pandey and F. Patella, J. Vac. Sci. Technol. ***15,*** 1252 (1978).

9. Angle-Resolved Photoemission Studies of Semiconductor Bulk and Surface States, D.E. Eastman, F.J. Himpsel, J.A. Knapp and K.C. Pandey, ***Physics of Semiconductors 1978,*** Inst. of Phys. Conf. Series 43, Bristol and London, 1059 (1979).

10. Quantum Photoyield of Diamond(111) - A Stable Negative Affinity Emitter, F.J. Himpsel, J.A. Knapp, J.A. VanVechten and D.E. Eastman, Phys. Rev. ***20***, 624 (1979).

11. Photoemission Studies of Intrinsic Surface States on Si(100), F.J. Himpsel and D.E. Eastman, J. Vac. Soc. Technol. ***16***, 1297 (1979).

12. Microscopic Compound Formation at the Pd/Si(111) Interface, J.L. Freeouf, G.W. Rubloff, P.S. Ho and T.S. Kuan, Phys. Rev. Lett. ***43***, 1836 (1979).

13. Silicide Schottky Barriers: An Elemental Description, J.L. Freeouf, Sol. St. Commun.***33***, 1059 (1980).

14. Geometrical and Electronic Structure of Si(001) and Si(111) Surfaces: A Status Report, D.E. Eastman, J. Vac. Sci. Technol. (in press).

B. Electronic structure of Group IV and Group III-V semiconductors.

15. Photoemission Spectroscopy Using Synchrotron Radiation. II The Electronic Structure of Germanium, W. D. Grobman, D. E. Eastman, and J. L. Freeouf, Phys. Rev. B*12*, 4405 (1975).

16. Angle-Resolved Photoemission and Valence Band Dispersion E ($\vec{k}$) for GaAs: Direct vs Indirect Models, T-C. Chiang, J.A. Knapp and D.E. Eastman, Sol. St. Commun. *31*, 917 (1979).

17. Angle-Resolved Photoemission, Valence Band Dispersions E($\vec{k}$), and Electron and Hole Lifetimes for GaAs, T.-C. Chiang, J.A. Knapp, M. Aono, and D.E. Eastman, Phys. Rev. (in press).

18. Experimental Energy Band Dispersions, Critical Points, and Spin-Orbit Splittings for GaSb Using Angle-Resolved Photoemission, T.-C. Chiang and D.E. Eastman, Phys. Rev. (in press).

C. Electronic structure of metal surfaces.

19. Observation of a Λ_1-symmetry Surface State on Ni(111), F. J. Himpsel and D. E. Eastman, Phys. Rev. Letters *41*, 507 (1978).

20. An Intrinsic Λ_1-Symmetry Surface State on Co(0001), F. J. Himpsel and D. E. Eastman, Phys. Rev. B*20*, 3217 (1979).

D. Electronic structure of metals and metallic compounds.

21. Electronic Structure of the Thorium Hydrides ThH_2 and Th_4H_{15}, J. H. Weaver, J. A. Knapp, D. E. Eastman, D. T. Peterson, and C. B. Satterhwaite, Phys. Rev. Letters *39*, 639 (1977).

22. Experimental Band Structure and Temperature-Dependent Magnetic Exchange Splitting of Nickel Using Angle-Resolved Photoemission, D. E. Eastman and F. J. Himpsel, Phys. Rev. Letters *40*, 1514 (1978).

23. Direct Determination of Lifetime and Energy Dispersion for the Empty Λ_1 Conduction D. E. Eastman, J. A. Knapp and F. J. Himpsel, Band of Copper, Phys. Rev. Lett., *41*, 825 (1978).

24. Experimental Energy Dispersion for Valence and Conduction Bands of Palladium, F. J. Himpsel and D. E. Eastman, Phys. Rev. *B18*, 5236 (1978).

25. Experimental Energy Band Dispersions and Exchange Splitting for Nickel, F. J. Himpsel, J. A. Knapp and D. E. Eastman, Phys. Rev. B*19*, 2919 (1979).

26. Experimental Energy Band Dispersions and Lifetimes for Valence and Conduction Bands of Copper using Angle-Resolved Photoemission, J. A. Knapp, F. J. Himpsel and D. E. Eastman, Phys. Rev. B*19*, 4952 (1979).

27. Temperature-Dependent Energy Band Dispersion of Surface and Bulk Bands of Copper using Angle-Resolved Photoemission, J. A. Knapp, F. J. Himpsel, A. R. Williams and D. E. Eastman, Phys. Rev. B*19*, 2844 (1979).

28. Symmetry Method for the Absolute Determination of Energy Band Dispersion $E(\vec{k})$ using Angle-Resolved Photoelectron Spectroscopy, Eberhard Dietz and D. E. Eastman Phys. Rev. Letters ***41***, 1674 (1978).

29. Experimental Band Dispersions E $(\vec{k})$ Along Three Main Symmetry Lines of LaB_6 Using Angle-Resolved Photoemission from a One Crystal Surface, M. Aono, T-C. Chiang, J.A. Knapp, T. Tanaka and D.E. Eastman, Sol. St. Commun. ***32***, 271 (1979).

31. Experimental Exchange-Split Energy Band Dispersions for Fe and Co, D.E. Eastman, F.J. Himpsel and J.A. Knapp, Phys. Rev. Lett. ***44***, 95 (1980).

32. Experimental Energy Band Dispersions and Magnetic Exchange Splitting for Cobalt, F.J. Himpsel and D.E. Eastman, Phys. Rev. (in press).

E. Studies of electronic many-electron effects.

32. Two-Electron Resonance at the 3p-Threshold of Cu and Ni, M. Iwan, F.J. Himpsel and D.E. Eastman, Phys. Rev. Lett. ***43***, 1829 (1979).

33. Observation of the Transition from the Adiabatic to the Sudden Regime for the $M_3M_{4,5}M_{4,5}(^1G)$ Auger Excitation in Zinc, F.J. Himpsel, D.E. Eastman, and E.E. Koch, Phys. Rev. Lett. ***44***, 214 (1980).

34. Resonant Photoemission Shake-Up and Auger Processes at the 3p Photothreshold in Ga and GaP, T.-C. Chiang and D.E. Eastman, Phys. Rev. (in press).

IV. BIOGRAPHY OF PRINCIPAL INVESTIGATOR

BIOGRAPHY:

Dean E. Eastman received his BS, MS and Ph. D. degrees in Electrical Engineering at M.I.T. in 1962, 1963, and 1965, respectively. He has held a National Merit Scholarship (1958 to 1962), National Science Foundation Cooperative Fellowship (1962-1963) and IBM Fellowship (1963-65). He is an IBM Fellow, and is also the manager of the Photoemission and Surface Physics Group at IBM. Currently he is Chairman of the Solid State Sciences Committee of the National Academy of Sciences, a Fellow of the American Physical Society, a member of the Users Executive Committee of the Synchrotron Radiation Center at the University of Wisconsin, a member of the National Science Foundation Advisory Committee for Condensed Matter Science, and a member of the Advisory Committee for the National Synchrotron Light Source Project, Brookhaven National Laboratory. He was a visiting Professor of Electrical Engineering at M.I.T. (1972-73 academic year). He is the co-recipient of the 1980 Buckley Prize of the American Physical Society. His interests include developing new photoemission spectroscopy techniques and applying them to a broad range of studies of the electronic band structure of solids and surfaces, chemisorption and semiconductor interfaces.

PUBLICATIONS OF DEAN E. EASTMAN

1. D. E. Eastman, Measurements of Third-Order Elastic Moduli of Yttrium Iron Garnet, J. Appl. Phys. ***37***, 2312 (1966).

2. D. E. Eastman, Second Order Magnetoelastic Properties of Yttrium Iron Garnet, J. Appl. Phys. ***37***, 966 (1966).

3. D. E. Eastman, Ultrasonic Study of First-Order and Second-Order Magnetoelastic Properties of Yttrium Iron Garnet, Phys. Rev. ***148***, 530 (1966).

4. D. E. Eastman, R. J. Joenk and D. T. Teaney, Antiferromagnetic Resonance in $RbMnF_3$ under Axial Stress, Phys. Rev. Letters ***17***, 300 (1966).

5. D. E. Eastman and M. W. Shafer, Antiferromagnetic Resonance in Cubic $TiMnF_3$, J. Appl. Phys. ***38***, 1274 (1967).

6. D. E. Eastman, Magnetoelastic Coupling in $RbMnF_3$, Phys. Rev. ***156***, 646 (1967).

7. D. E. Eastman and M. W. Shafer, Magnetostriction in Ferromagnetic $CdCr_2Se_4$, J. Appl. Phys. ***38***, 4761 (1967).

8. D. E. Eastman, M. W. Shafer and R. Figat, Cobalt-Doped $TlMnF_3$, A Zero Anisotropy Cubic Antiferromagnetic, J. Appl. Phys. ***38***, 5209 (1967).

9. D. E. Eastman, Temperature Dependence of the Resonance Linewidth in EuO, Phys. Letters ***28A***, 136 (1968).

10. D. E. Eastman and W. F. Krolikowski, New Photoemission Studies of the d-bands of Nickel and Copper, Phys. Rev. Letters ***21***, 623 (1968).

11. D. E. Eastman, Photoemission Studies of the Electronic Structure of Transition Metals, J. Appl. Phys. ***40***, 1387 (1969).

12. D. E. Eastman, F. Holtzberg and S. Methfessel, Photoemission Studies of the Electronic Structure of EuO, EuS, EuSe and GdS, Phys. Rev. Letters ***23***, 226 (1969).

13. S. Methfessel, D. E. Eastman, F. Holtzberg, T. R. McGuire, T. Penney, M. W. Shafer and S. von Molnar, Magnetic, Electric and Optical Properties of Rare Earth Chalcogenides, Proc. of the Rare Earth Conference, Grenoble, France, Compte Rendus ***180***, 565 (1970).

14. D. E. Eastman, Hot Electron Scattering and Optical Density of States in Yttrium, Sol. St. Commun. ***8***, 41 (1970).

15. D. E. Eastman, Photoemission Studies of d-Band Structure in Sc, Y, Gd, Ti, Zr, Hf, V, Nb, Cr, and Mo, Sol. State Commun. *7*, 1697 (1970).

16. D. E. Eastman, Photoemission Studies of Scandium, Titanium and Zirconium, ***Electronic Density of States***, L. H. Bennett, editor, NBS Special Publ. 323 (1971), p. 205.

17. J. F. Janak, D. E. Eastman, and A. R. Williams, Direct-Transition Analysis of Photoemission from Palladium, ***Electronic Density of States***, L. H. Bennett, editor, NBS Special Publ. 323 (1971), p. 181.

18. J. F. Janak, D. E. Eastman and A. R. Williams, Direct-Transition Analysis of New Photoemission Data for Palladium, Sol. State Commun. ***8***, 271 (1970).

19. D. E. Eastman and J. K. Cashion, Photoemission from Cu, Ag and Au in the 10- to 27-eV Energy Range, Phys. Rev. Letters ***24***, 310 (1970).

20. D. E. Eastman, Photoemission Work Functions of Transition, Rare-Earth, and Noble Metals, Phys. Rev. B ***2***, 1 (1970).

21. D. E. Eastman and J. J. Donelon, High Intensity Hot Filament Vacuum Ultraviolet Light Source, Rev. Sci. Instruments ***41***, 1648 (1970).

22. D. E. Eastman, Photoemission from Ni, Co and Fe from 10 to 41 eV, Proceedings of 1970 International Magnetism Conference at Grenoble, France, Sept. 1970, J. de Physique ***32***, Colloque C1, 293 (1971).

23. D. E. Eastman, Lack of Evidence for Intrinsic Surface States in Ni and Cu, Phys. Rev. B ***3***, 1769 (1971).

24. R. J. Gambino, D. E. Eastman, T. R. McGuire, V. L. Moruzzi, and W. D. Grobman, Evidence of the Intrinsic Metallic Character of Some Rare Earth Pnictides, J. Appl. Phys. ***42***, 1468 (1971).

25. D. E. Eastman and Moshe Kuznietz, Photoemission Studies of f-states and Valence Bands in Several Rare Earth and Uranium Compounds, J. Appl. Phys. ***42***, 1396 (1971).

26. D. E. Eastman and Moshe Kuznietz, Energy-Dependent Photoemission Intensities of "f" States in EuS, GdS, and US, Phys. Rev. Letters 26, 846 (1971).

27. D. E. Eastman, Photoemission Spectra for Liquid and Crystalline Au, Phys. Rev. Letters ***26***, 1108 (1971).

28. D. E. Eastman, J. K. Cashion and A. C. Switendick, Photoemission Studies of Energy Levels in the Palladium—Hydrogen System, Phys. Rev. Letters ***27***, 35 (1971).

29. J. K. Cashion, J. L. Mees, D. E. Eastman, J. A. Simpson and C. E. Kuyatt, Windowless Photoelectron Spectrometer for High Resolution Studies of Solids and Surfaces, Rev. Sci. Instruments ***42***, 1670 (1971).

30. D. E. Eastman and J. K. Cashion, Photoemission Energy Level Measurements of Chemisorbed CO and O on Ni, Phys. Rev. Letters ***27***, 1520 (1971).

31. D. E. Eastman, Ultraviolet Photoelectron Spectroscopy Studies of Noble and Transition Metals, ***Electron Spectroscopy***, D. Shirley, editor, North Holland, 1972, pp. 487–514.

32. T. H. Di Stefano and D. E. Eastman, The Band Edge of Amorphous SiO_2 by Photoinjection and Photoconductivity Measurements, Sol. State Comm. ***9***, 2259 (1971).

33. T. H. Di Stefano and D. E. Eastman, Photoemission Measurements of the Valence Levels of Amorphous SiO_2, Phys. Rev. Letters ***27***, 1560 (1971).

34. D. E. Eastman, Photoemission Spectroscopy of Metals, Chapter in ***Technique of Metals Research VI***, E. Passaglia, editor, Interscience (1972), pp. 413—479.

35. D. E. Eastman and A. R. Williams, Photoemission Studies of the Electronic Structure of Solids, ***Computational Solid State Physics***, ed. by F. Herman, N. W. Dalton, and T. R. Kohler, Plenum, 1972 pp. 23—42.

36. D. E. Eastman, Photoemission Energy Level Measurements of Sorbed Gases on Titanium, Sol. State Commun. ***10***, 933 (1972).

37. W. D. Grobman and D. E. Eastman, Temperature—Modulated Photoemission Spectra for Gold, Phys. Rev. Letters ***28***, 1038 (1972).

38. D. E. Eastman and W. D. Grobman, Photoemission Energy Distributions for Au from 10 to 40 eV Using Synchrotron Radiation, Phys. Rev. Letters ***28***, 1327 (1972).

39. D. E. Eastman and W. D. Grobman, Photoemission Densities of Intrinsic Surface States for Si, Ge and GaAs, Phys. Rev. Letters ***28***, 1378 (1972).

40. J. M. Baker and D. E. Eastman, Photoemission Spectra from Adsorbed O on W(110) and CO on W(100), J. Vac. Soc. ***10***, 223 (1973).

41. W. D. Grobman and D. E. Eastman, Photoemission Valence Band Densities of States for Si, Ge and GaAs Using Synchrotron Radiation, Phys. Rev. Letters ***29***, 1508 (1972).

42. D. E. Eastman and W. D. Grobman, Photoemission Studies of Si, Ge and GaAs Using Synchrotron Radiation in the 7—25 eV Range, Proc. of 11th International Semiconductor Conference at Warsaw, Poland (Polish Scientific Publishers), 889 (1972).

43. W. D. Grobman and D. E. Eastman, Modulated Photoemission Spectroscopy: Application to Gold, Proc. of 1st International Conference on Modulation Spectroscopy, Surface Science ***37***, 355 (1973).

44. D. E. Eastman and W. D. Grobman, Photoemission Observations of Resonant d-Levels and d-band Formation for Very Thin Overlayers of Cu and Pd on Ag, Phys. Rev. Letters ***30***, 177 (1973).

45. W. D. Grobman, D. E. Eastman and M. L. Cohen, A Relationship Between Photoemission—Determined Valence Band Gaps in Semiconductors and Insulators and Ionicity-Parameters, Physics Letters ***43A***, 49 (1973).

46. P. O. Nilsson and D. E. Eastman, Photoemission Anisotropy Studies for Ag(111) and Ag(100) Single Crystal Films, Physica Scripta, ***8***, 113 (1973).

47. J. Freeouf, M. Erbudak and D. E. Eastman, Photoemission Spectra for Gold for 15 &ll. hν &ll. 90 eV and the X-Ray Limit, Sol. St. Commun. ***13***, 771 (1973).

48. P. O. Nilsson, G. Arbman and D. E. Eastman, Measurements and Calculations of Photoemission from Ca, Sol. St. Commun. ***12***, 627 (1973).

49. D. E. Eastman, Photoemission Spectroscopy Using Synchrotron Radiation, Proc. of the Brookhaven Synchrotron Radiation Study Symposium, BNL 50381, pp. 31—35, June, 1973.

50. D. E. Eastman, J. Freeouf and M. Erbudak, Photoemission Overviews of Valence Band Densities of States for Ge, GaAs, GaP, InSb, ZnSe and CdTe Using Synchrotron Radiation, J. de Physique, Suppl. C6, 1973, p. C6—37.

51. D. E. Eastman and J. Freeouf, Valence Band and Core Level Studies of InSb via Photoemission Measurements in the 20—70 eV Range, Sol. St. Commun., ***13***, 18185 (1973).

52. D. E. Eastman, Quasielastic Electron Scattering in EuO: A Possible Explanation for the Observed "Paramagnetic" Spin-Polarized Photoemission, Phys. Rev. ***B8***, 6027 (1973).

53. D. E. Eastman, J. E. Demuth and J. M. Baker, Application of Ultraviolet Photoemission Spectroscopy to Surface Studies (Extended abstract of invited talk presented at the 20th National Symposium of the American Vacuum Society, J. Vac. Sci. Technol. ***11***, 273 (1974).

54. W. D. Grobman, R. A. Pollak, D. E. Eastman, E. T. Maas, Jr. and B. A. Scott, Valence Electronic Structure and Charge Transfer in TTF—TCNQ from Photoemission Spectroscopy, Phys. Rev. Letters ***32***, 534 (1974).

55. E. K. Li, K. H. Johnson, D. E. Eastman and J. L. Freeouf, Localized and Bandlike Valence—Electron States in FeS_2 and NiS_2, Phys. Rev. Letters ***32***, 470 (1974).

56. D. E. Eastman, W. D. Grobman, J. L. Freeouf, and M. Erbudak, Photoemission Spectroscopy Using Synchrotron Radiation I. Overviews of Valence Band Structure for Ge, GaAs, GaP, InSb, ZnSe, CdTe and AgI, Phys. Rev., ***B9***, 3473 (1974).

57. D. E. Eastman, F. Holtzberg, J. Freeouf and M. Erbudak, Photoemission Studies of Valence Bands and 4f Multiplet Structure in NdS, SmS, EuS, GdS, DyS, and ErS, 19th Conf. on Magnetism and Magnetic Materials, Boston, Mass., Nov. 1973 AIP Conf. Proc. ***18***, 1030 (1974).

58. T. R. McGuire, W. D. Grobman and D. E. Eastman, Photoemission Studies of Ni—Co Alloys Having Large Anisotropic Magnetoresistance, 19th Conf. on Magnetism and Magnetic Materials, Boston, Mass., Nov. 1973 AIP Conf. Proc. ***18***, 903 (1974).

59. D. E. Eastman, J. L. Freeouf and M. Erbudak, Valence and Conduction Band State Densities of Crystalline and Amorphous Ge As seen Via Photoelectron Spectroscopy, Tetrahedrally Bonded Amorphous Semiconductor Conference, IBM, Yorktown Heights, NY, March 1974, AIP Conf. Proc. ***20***, 95 (1974).

60. J. E. Demuth and D. E. Eastman, Photoemission Observations of π—d Bonding and Surface Reactions of Adsorbed Hydrocarbons on Ni(111), Phys. Rev. Letters, ***32***, 1123 (1974).

61. D. E. Eastman and J. E. Demuth, Photoemission Studies of Inorganic (Co,O,NO) and Organic (C_2H_2,C_2H_4,C_6H_6) Adsorbates on Ni(111) and Surface Reactions, Second International Conference on Solid Surfaces (invited paper), Kyoto, Japan, March 1974, Jap. J. of Appl. Phys. Suppl. 2, Pt. 2, 827 (1974).

62. R. A. Pollak, F. Holtzberg, J. L. Freeouf and D. E. Eastman, Temperature and Composition-Dependent Valence Mixing of Sm in Cation- and Anion-Substituted SmS Observed by X-Ray Photoemission Spectroscopy (XPS), Phys. Rev. Letters, ***33***, 820 (1974).

63. D. E. Eastman and J. L. Freeouf, Photoemission Partial Yield Measurements of Unoccupied Intrinsic Surface States for Ge(111) and GaAs(110), Phys. Rev. Letters ***33***, 1601 (1974).

64. P. J. Feibelman and D. E. Eastman, Photoemission Spectroscopy — Correspondence between Quantum Theory and Phenomenology, Phys. Rev. B ***10***, 4392 (1974).

65. D. E. Eastman, A Survey of Photoemission Measurements Using Synchrotron Radiation in the $5 \leq \hbar \leq 100$ eV Range, Proc. of the IV International Conf. on Vacuum Ultraviolet Radiation Physics, Hamburg, July 1974 (pp. 417—449).

66. D. E. Eastman and J. L. Freeouf, Photoemission Partial State Densities of Overlapping p— and d—states for NiO, CoO, FeO, MnO, and Cr_2O_3, Phys. Rev. Lett. ***34***, 395 (1974).

67. D. E. Eastman and J. E. Demuth, Photoemission Studies of Inorganic (CO,O,NO) and Organic (C_2H_2,C_2H_4,C_6H_6) Adsorbates on Ni(111) and Surface Reactions, Japanese J. of Appl. Phys. Supp. 2, pt. 2, 827 (1974).

68. W. D. Grobman, D. E. Eastman, J. L. Freeouf and J. Shaw, Valence and Conduction Band Structure of Ge Using Theoretical and Experimental Photoemission Spectra from 6.5 to 23 eV, Proc. XII Int. Conf. on the Phys. of Semicond., July 1974 (B. G. Teubner, Stuttgart, 1974).

69. W. D. Grobman and D. E. Eastman, Absolute Conduction— and Valence—Band Positions for Ge from an Anisotropic Model of Photoemission, Phys. Rev. Letters ***33***, 1034 (1974).

70. J. L. Freeouf, D. E. Eastman, W. D. Grobman, F. Holtzberg and J. B. Torrance, Spectroscopically Observed Valence Mixing in SmS and Related Compounds, Phys. Rev. Letters ***33***, 161 (1974).

71. T. Gustafsson, E. W. Plummer, D. E. Eastman, and J. L. Freeouf, Interpretation of the Photoelectron Spectra of Molecularly Adsorbed CO, Sol. St. Commun. ***17***, 391 (1975).

72. J. L. Freeouf and D. E. Eastman, Photoemission Measurements of Filled and Empty Surface States and their Relation to Schottky Barriers, Critical Reviews in Solid State Science ***5***, 245 (1975).

73. D. E. Eastman and J. L. Freeouf, Relation of Schottky Barriers to Empty Surface States on III-V Semiconductors, Phys. Rev. Letters *34*, 1624 (1975).

74. W. J. Pardee, G. D. Mahan, D. E. Eastman, R. A. Pollak, L. Ley, F. R. Mc Feely, S. P. Kowalczyk, and D. A. Shirley, Analysis of Surface— and Bulk—plasmon Contributions to X-Ray Photoemission Spectra, Phys. Rev. B*11*, 3614 (1975).

75. D. E. Eastman and M. I. Nathan, Photoelectron Spectroscopy, Physics Today *28* (1975).

76. G. W. Bancroft, I. Adams, J. K. Creber, D. E. Eastman and W. Gudat, High Resolution Photoelectron Studies: Electric Field Ambient Splittings of Cd and Sn 4d Energy Levels in Organometallic Compounds, Chem. Phys. Letters *38*, 83 (1976).

77. J. E. Demuth and D. E. Eastman, Determination of the State of Hybridization of Unsaturated Hydrocarbons Chemisorbed on Nickel, Phys. Rev. B *13*, 1523 (1976).

78. J. E. Demuth and D. E. Eastman, The Application of UPS to the Study of Chemisorption, J. Vac. Sci. and Technol. *13*, 283 (1976).

79. Peter J. Feibelman and D. E. Eastman, Angle-of-Incidence Dependence of Photoemission of a Localized Electron from a Jellium Solid, Phys. Rev. Letters (Comment) *36*, 234 (1976).

80. W. Gudat, D. E. Eastman, and J. L. Freeouf, Empty Surface States on Semiconductors: Their Interactions with Metal Overlayers and their Relation to Schottky Barriers, J. Vac. Sci. Technol. *13*, 250 (1976).

81. E. Spiller, R. Feder, J. Topalian, D. E. Eastman, W. Gudat, and D. Sayre, X-Ray Microscopy of Biological Objects with Carbon K_c and with Synchrotron Radiation, Science *191*, 1172 (1976).

82. W. D. Grobman, D. E. Eastman, and J. L. Freeouf, Photoemission Spectroscopy Using Synchrotron Radiation. II The Electronic Structure of Germanium, Phys. Rev. B*12*, 4405 (1975).

83. E. Spiller, R. Feder, J. Topalian, W. Gudat and D. E. Eastman, X-Ray Lithography with Synchrotron Radiation, 7th International Conference on Electron and Ion Beam Science and Technology, 233 (1976).

84. J. E. Demuth and D. E. Eastman, Photoemission Observation of Two Molecular Phases of CO Adsorbed on Cu(100), Solid St. Comm. 18, 1487 (1976).

85. W. Gudat and D. E. Eastman, Electronic Surface Properties of III-V Semiconductors: Excitonic Effects, Band-Bending Effects, and Interactions with Au and O Adsorbate Layers, J. Vac. Sci. Technol. 13, 831 (1976).

86. E. Spiller, D. E. Eastman, R. Feder, W. D. Grobman, W. Gudat and J. Topalian, Application of Synchrotron Radiation to X-Ray Lithography, J. Appl. Phys. *47*, 5450 (1976).

87. P. S. Bagus, J. L. Freeouf and D. E. Eastman, Relative Intensities for Multiplet and Crystal—field—split Transition—Metal—Ion Photoemission Spectra, Phys. Rev. B *15*, 3661 (1977).

88. D. E. Eastman, Comments on XUV Photoelectron Spectroscopy User Needs, Proc. of Quebec Summer Workshop on Synchrotron Radiation Facilities, 15—18 June 1976, Quebec, Canada, p4—33.

89. G. M. Bancroft, T. K. Sham, D. E. Eastman and W. Gudat, Photoelectron Spectra of Solid Inorganic Compounds Using Synchrotron Radiation: Valence Band Spectra and Ligand Field Broadening of Core d Levels, J. Am. Chem. Soc. *99*, 1752 (1977).

90. G. M. Bancroft, W. Gudat, and D. E. Eastman, Photoemission Studies of the Pb 5d, Sn 4d and In 4d Lines using Synchrotron Radiation, J. Elect. Spect. and Related Phenomena, *10*, 407 (1977).

91. E. W. Plummer, T. Gustafsson, W. Gudat and D. E. Eastman, Partial Photoionization Cross Sections of N_2 and CO Using Synchrotron Radiation, Phys. Rev. A *15*, 2339 (1977).

92. K. C. Pandey, J. L. Freeouf, and D. E. Eastman, Photoemission and Band-Structure Studies of the GaAs(110) Surface, J. Vac. Sci. Technol. *14*, 904 (1977).

93. J. H. Weaver, J. A. Knapp, D. E. Eastman, D. T. Peterson, and C. B. Satterhwaite, Electronic Structure of the Thorium Hydrides ThH_2 and Th_4H_{15}, Phys. Rev. Letters *39*, 639 (1977).

94. W. Gudat and D. E. Eastman, Photoemission from Semiconductor Surfaces, Chapter in ***Photoemission and the Electronic Properties of Surfaces***, Edited by B. Feurbacher, B. Fitton, and R. F. Willis, April 1978.

95. T. Gustafsson, E. W. Plummer, D. E. Eastman and W. Gudat, Partial Photoionization Cross Sections of CO_2 Between 20 and 40 eV Studied with Synchrotron Radiation, Phys. Rev. *A*, 175 (1978).

96. J. A. Knapp, D. E. Eastman, K. C. Pandey, and F. Patella, Surface Electronic Structure Studies of GaAs(110), J. Vac. Sci. Technol. *15*, 1252 (1978).

97. D. E. Eastman and F. J. Himpsel, Experimental Band Structure and Temperature-Dependent Magnetic Exchange Splitting of Nickel Using Angle-Resolved Photoemission, Phys. Rev. Letters *40*, 1514 (1978).

98. F. J. Himpsel and D. E. Eastman, Observation of a Λ_1-symmetry Surface State on Ni(111), Phys. Rev. Letters *41*, 507 (1978).

99. D. E. Eastman, J. A. Knapp and F. J. Himpsel, Direct Determination of Lifetime and Energy Dispersion for the Empty Λ_1 Conduction Band of Copper, Phys. Rev. Lett., *41*, 325 (1978).

100. G. Aeppli, J. J. Donelon, D. E. Eastman, R. W. Johnson, R. A. Pollak and H. J. Stolz, Addition of Monochromated UV Discharge Lamp to X-Ray Photoemission Spectrometer, Journal of Elec. Spec. and Related Phenomena *14*, 121 (1978).

101. G. M. Bancroft, W. Gudat and D. E. Eastman, Photoionization-Cross-Section Studies of Atomic and Final-State Effects on the Pb 5d Core Levels using Synchrotron Radiation, Phys. Rev. ***B17***, 4499 (1978).

102. F. J. Himpsel and D. E. Eastman, Experimental Energy Dispersion for Valence and Conduction Bands of Palladium, Phys. Rev. ***B18***, 5236 (1978).

103. Eberhard Dietz and D. E. Eastman, A Symmetry Method for the Absolute Determination of Energy Band Dispersion $E(\vec{k})$ using Angle-Resolved Photoelectron Spectroscopy, Phys. Rev. Letters ***41***, 1674 (1978).

104. D.E. Eastman, Photoelectron Spectroscopy, in ***Encyclopedia of Physics***, G.L. Trigg, Editor, (in press 1980).

105. D. E. Eastman, F. J. Himpsel, J. A. Knapp and K. C. Pandey, Angle-Resolved Photoemission Studies of Semiconductor Bulk and Surface States, ***Physics of Semiconductors 1978***, Inst. of Phys. Conf. Series 43, Bristol and London, 1059 (1979).

106. F. J. Himpsel, J. A. Knapp and D. E. Eastman, Experimental Energy Band Dispersions and Exchange Splitting for Nickel, Phys. Rev. ***B19***, 2919 (1979).

107. J. A. Knapp, F. J. Himpsel and D. E. Eastman, Experimental Energy Band Dispersions and Lifetimes for Valence and Conduction Bands of Copper using Angle-Resolved Photoemission, Phys. Rev. ***B19***, 4952 (1979).

108. J. A. Knapp, F. J. Himpsel, A. R. Williams and D. E. Eastman, Temperature-Dependent Energy Band Dispersion of Surface and Bulk Bands of Copper using Angle-Resolved Photoemission, Phys. Rev. ***B19***, 2844 (1979).

109. F.J. Himpsel, J.A. Knapp and D.E. Eastman, Angle-Resolved Photoemission Study of the Electronic Structure of Chemisorbed Hydrogen on Ni(111), Phys. Rev. ***B19***, 2872 (1979).

110. F. J. Himpsel and D. E. Eastman, An Intrinsic Λ_1-Symmetry Surface State on Co(0001), Phys. Rev. ***B20***, 3217 (1979).

111. F. J. Himpsel, J. A. Knapp, J. A. VanVechten and D. E. Eastman, Quantum Photoyield of Diamond(111) - A Stable Negative Affinity Emitter, Phys. Rev. ***B20***, 624 (1979).

112. F. J. Himpsel and D. E. Eastman, Photoemission Studies of Intrinsic Surface States on Si(100), J. Vac. Soc. Technol. ***16***, 1297 (1979).

113. T-C. Chiang, J.A. Knapp and D.E. Eastman, Angle-Resolved Photoemission and Valence Band Dispersion $E(\vec{k})$ for GaAs: Direct vs Indirect Models, Sol. State Comm. ***31***, 917 (1979).

114. M. Aono, T-C. Chiang, J.A. Knapp, T. Tanaka and D.E. Eastman, Experimental Band Dispersions $E(\vec{k})$ Along Three Main Symmetry Lines of LaB_6 Using Angle-Resolved Photoemission from a One Crystal Surface, Sol. State Commun. ***32***, 271 (1979).

115. D.E. Eastman, J.J. Donelon, N.C. Hien and F.J. Himpsel, An Ellipsoidal Mirror Display Analyzer System for Electron Energy and Angular Measurements, Nuclear Instrum. & Methods (in press).

116. D.E. Eastman, F.J. Himpsel and J.A. Knapp, Experimental Exchange-Split Energy Band Dispersions for Fe and Co, Phys. Rev. Lett. ***44***, 95 (1980).

117. M. Iwan, F.J. Himpsel and D.E. Eastman, Two-Electron Resonance at the 3p-Threshold of Cu and Ni, Phys. Rev. Lett. ***43***, 1829 (1979).

118. D.E. Eastman, R.V. Coleman, J.F. Janak, G. Wendin and A.R. Williams, Electronic Structure of Magnetic 3d Metals: Ground State, Fermi Surface, and Photoemission Properties, J. Appl. Phys. (in press).

119. D.E. Eastman, Geometrical and Electronic Structure of Si(001) and Si(111) Surfaces: A Status Report, J. Vac. Sci. Technol. (in press).

120. T.-C. Chiang, J.A. Knapp, M. Aono, and D.E. Eastman, Angle-Resolved Photoemission, Valence Band Dispersions $E(\vec{k})$, and Electron and Hole Lifetimes for GaAs, Phys. Rev. (in press).

121. T.-C. Chiang and D.E. Eastman, Experimental Energy Band Dispersions, Critical Points, and Spin-Orbit Splittings for GaSb Using Angle-Resolved Photoemission, Phys. Rev.(in press).

122. F.J. Himpsel and D.E. Eastman, Experimental Energy Band Dispersions and Magnetic Exchange Splitting for Cobalt, Phys. Rev. (in press).

123. F.J. Himpsel, D.E. Eastman, and E.E. Koch, Observation of the Transition from the Adiabatic to the Sudden Regime for the $M_3M_{4,5}M_{4,5}(^1G)$ Auger Excitation in Zinc, Phys. Rev. Lett. ***44***, 214 (1980).

124. T.-C. Chiang and D.E. Eastman, Resonant Photoemission Shake-Up and Auger Processes at the 3p Photothreshold in Ga and GaP, Phys. Rev. (in press).

125. J.F. van der Veen, F.J. Himpsel and D.E. Eastman, Structure-Dependent 4f Core Level Binding Energies for Surface Atoms on Ir(111), Ir(100)-(5×1), Phys. Rev. Lett. ***44***, 189 (1980).

126. G. Kaindl, T.-C. Chiang, D.E. Eastman, F.J. Himpsel, Distance-Dependent Relaxation Shifts of Photoemission and Auger Energies for Xe on Pd(001), submitted to Phys. Rev. Lett.

127. J.F. van der Veen, F.J. Himpsel, D.E. Eastman, and P. Heimann, Angular Dependent Photon-Stimulated Desorption of Ions from a $V_2O_5(010)$ Surface, submitted to Sol. St. Commun.

128. M. Aono, F.J. Himpsel, and D.E. Eastman, Experimental Band Structure $E(\vec{k})$ of V_3Si by Angle Resolved Photoemission, submitted to Phys. Rev. Lett.

129. D.E. Eastman, F.J. Himpsel, and J.F. van der Veen, Similarity Between the Si(111)-(7×7) and Impurity-Stabilized Si(111)-(1×1) Surfaces, submitted to Sol. St. Commun.

130. F.J. Himpsel, J.F. van der Veen, and D.E. Eastman, Experimental Bulk Energy Bands for Diamond Using $h\nu$-Dependent Photoemission, submitted to Phys. Rev. Lett.

131. A. Bradshaw, J.F. van der Veen, F.J. Himpsel, and D.E. Eastman, Electronic Properties of the Clean and Hydrogen-Covered TiC(111) Ti-Terminated Polar Surface, submitted to Sol. St. Commun.

132. M. Aono, T.-C. Chiang, J.A. Knapp, T. Tanaka, and D.E. Eastman, Direct Recombination and Auger Deexcitation Channels of La4d 4f Resonant Excitations in LaB_6, Phys. Rev. (in press).